PROCEEDINGS OF SPIE

SPIEDigitalLibrary.org/conference-proceedings-of-spie

The assembly and alignment of the 4MOST wide field corrector

Mark Cunningham, Peter Doel, David Brooks, Joar Brynnel, Roelof de Jong, et al.

Mark Cunningham, Peter Doel, David Brooks, Joar Brynnel, Roelof de Jong, Steffen Frey, Michael Schroeck, Miklos Gaebler, Daniel Sablowski, Michael Lehmitz, Greg Smith, Sam C. Barden, "The assembly and alignment of the 4MOST wide field corrector," Proc. SPIE 12184, Ground-based and Airborne Instrumentation for Astronomy IX, 121846V (29 August 2022); doi: 10.1117/12.2629247

SPIE.

Event: SPIE Astronomical Telescopes + Instrumentation, 2022, Montréal, Québec, Canada

The assembly and alignment of the 4MOST Wide Field Corrector

Mark Cunningham[a], Peter Doel[a], David Brooks[a], Joar Brynnel[b], Roelof de Jong[b], Steffen Frey[b], Michael Schroeck[b], Miklos Gaebler[b], Daniel Sablowski[b], Michael Lehmitz[c], Greg Smith[b], and Sam C. Barden[d]

[a]University College London, Gower St, WC1E 6BT, London, United Kingdom
[b]Leibniz Institute for Astrophysics Potsdam, An der Sternwarte 16, 14482 Potsdam, Germany
[c]Max-Planck-Institut fur Astronomie, Königstuhl 17, 69117 Heidelberg, Germany
[d]Canada France Hawaii Telescope, 65-1238 Mamalahoa Hwy Kamuela, Hawaii, United States

ABSTRACT

The 4-metre Multi-Object Spectroscopic Telescope (4MOST) is a fibre-fed multi-object spectrograph for the VISTA telescope at the ESO Paranal Observatory in Chile. The goal of the 4MOST project is to create a general-purpose and highly efficient spectroscopic survey facility for astronomers in the 4MOST consortium and the ESO community. The instrument itself will record 2436 simultaneous spectra over a $\sim$4.2 square degree field of view and consists of an optical Wide-Field Corrector (WFC), a fibre positioner system based on a tilting spine design, and three spectrographs giving both high and low spectral dispersion. The WFC comprises of 6 lenses grouped into 4 elements, 2 of which are cemented doublets that act as an atmospheric dispersion corrector (ADC). The first lens element is 0.9m in diameter whilst the diameter of the other elements is 0.65m. For the instrument to meet its science goals, each lens needs to be aligned to $\sim 50\mu m$ – a major challenge. This is achieved using contact metrology methods supplemented by pencil beam laser probes. In particular, a novel off-axis laser beam system has been implemented to test the optics' alignment before and after shipment. This paper details the alignment and assembly methods and presents the latest results on the achieved lens positioning and projected performance of the WFC.

Keywords: Wide-field multi-object spectrograph facility – VISTA telescope – Wide Field Corrector – 4MOST

1. INTRODUCTION

Spectroscopy will always be fundamental when it comes to ground-based astronomy, yielding unique astrophysical insights such as the chemical composition and nature of stellar populations in nearby galaxies along with accurate red-shifts and the ionizing radiation field of extra-galactic sources.[1] As technology and engineering continue to make great leaps, it is of no surprise that in the last decade there have been incredible strides in optical and infra-red imaging, with follow-up spectroscopy and telescope updates and reconfiguration becoming the status-quo. This has lead to large investment into Multi-Object Spectroscopic facilities. As the name suggests, Multi-Object Spectroscopy (MOS) is used to obtain simultaneous spectra of many objects. MOS uses multiple slits, mirrors, or optical fibres at the focal plane, to separate the light of many astronomical objects within a single field of view for spectral analysis. They allow multiple individually resolved spectra to be obtained per exposure and as such are ideal instruments for efficient large-scale, wide-field spectroscopic surveys. One such instrument is the 4-metre Multi-Object Spectroscopic Telescope (4MOST).

4MOST is a new spectroscopic survey facility that will provide the highest target multiplex on the largest field-of-view (FoV) in the Southern Hemisphere. The instrument is to be installed on the 4.1m Visible and Infrared Survey Telescope for Astronomy (VISTA) of the European Southern Observatory (ESO), located at

Further author information: (Send correspondence to Mark Cunningham)
E-mail: mark.cunningham.20@ucl.ac.uk

Ground-based and Airborne Instrumentation for Astronomy IX, edited by Christopher J. Evans, Julia J. Bryant, Kentaro Motohara, Proc. of SPIE Vol. 12184, 121846V
© 2022 SPIE · 0277-786X · doi: 10.1117/12.2629247

the Paranal Observatory in Chile. The instrument will complement and enhance the results of many large-area sky surveys, such as four space-based observatories of prime European interest: Gaia, eROSITA, Euclid, and PLATO, and many ground-based facilities like VST, DESI, Rubin Observatory, and SKA. The science programme of the 4MOST consortium is structured into ten surveys, each pursuing different science cases; five dedicated to Galactic Archaeology and five dedicated to Extra-galactic objects, including one of the most complete spectroscopic surveys of Active Galactic Nuclei (AGN) ever undertaken.[2]

In order for the project to carry out its ambitious science goals the optical performance of the instrument is critical. This places tight tolerances on the manufacture and alignment of the WFC optics. In particular precise micrometre scale alignment is required, a major challenge in any astronomical instrument assembly. In this paper, we outline the metrology methods used to precisely measure the elements of the WFC and present the results of the alignment and assembly of the WFC lenses along with the processes used.

1.1 Instrument overview

4MOST will provide a multiplex and spectral resolution, high enough to detect chemical and kinematic substructure in the stellar halo, bulge, and disks of the Milky Way, and enough wavelength coverage to secure receding velocities of extra-galactic objects over a large range in red-shift.[3] A new Wide Field Corrector (WFC) creates a 4.2 square degree FoV on the focal surface, where 2436 optical fibres positioned by the Australian–European Southern Observatory Positioner (AESOP) lead the light to two resolution $R{\sim}5000$ spectrographs and one $R{\sim}20{,}000$ spectrograph. This will yield more than 20 million spectra at resolution $R{\sim}5000$ (λ=370–950 nm) and more than 2 million spectra at $R{\sim}20,000$ (λ= 392.6-435.5, 516-573, 610-679 nm) over the duration of the surveys conducted by 4MOST.[2] A metrology system supports the accurate positioning of the fibres in the focal surface, while a calibration system provides the illumination from the M2 support spiders for wavelength and flat-field calibration. Figure 1 and 2 show in detail the 4MOST instrument including the WFC.

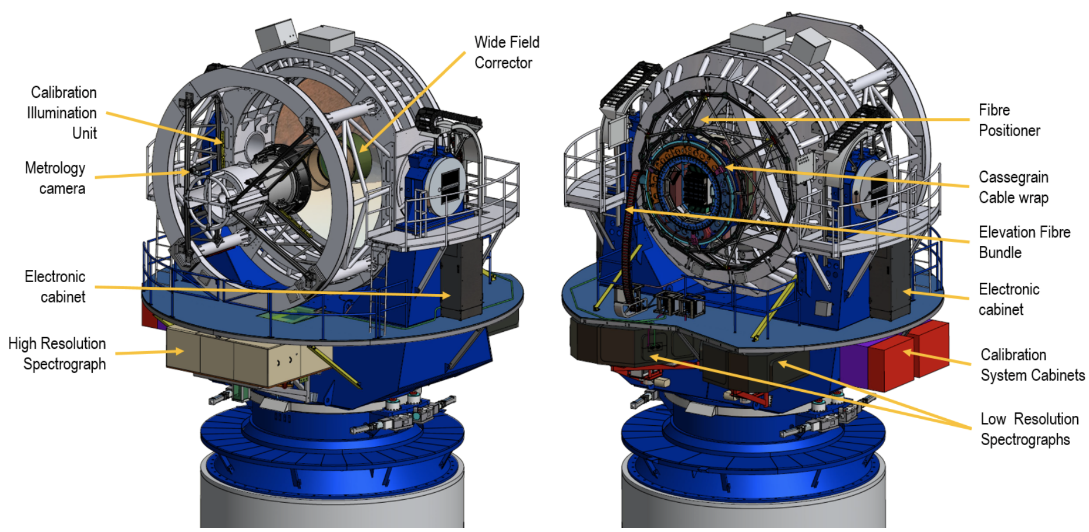

Figure 1: Physical layout of the new 4MOST elements on the VISTA telescope describing each part of the instrument in detail as viewed from the front and back. (Image credit: 4MOST consortium)

1.2 Optical Design

The WFC is a key optical component for the 4MOST facility in that it performs the critical image correction to the VISTA telescope optics in order to deliver the requisite field of view, image quality and plate scale; all of which are crucial for the science cases.[4] The WFC consists of 6 lenses grouped in 4 parts, two of which act as doublets that make up the Atmospheric Disperson Corrector (ADC) unit. The positions of the lenses are shown in Figure 3, labelled L1, L2, L3 and L4. The lenses were manufactured at KiwiStar Optics, New Zealand

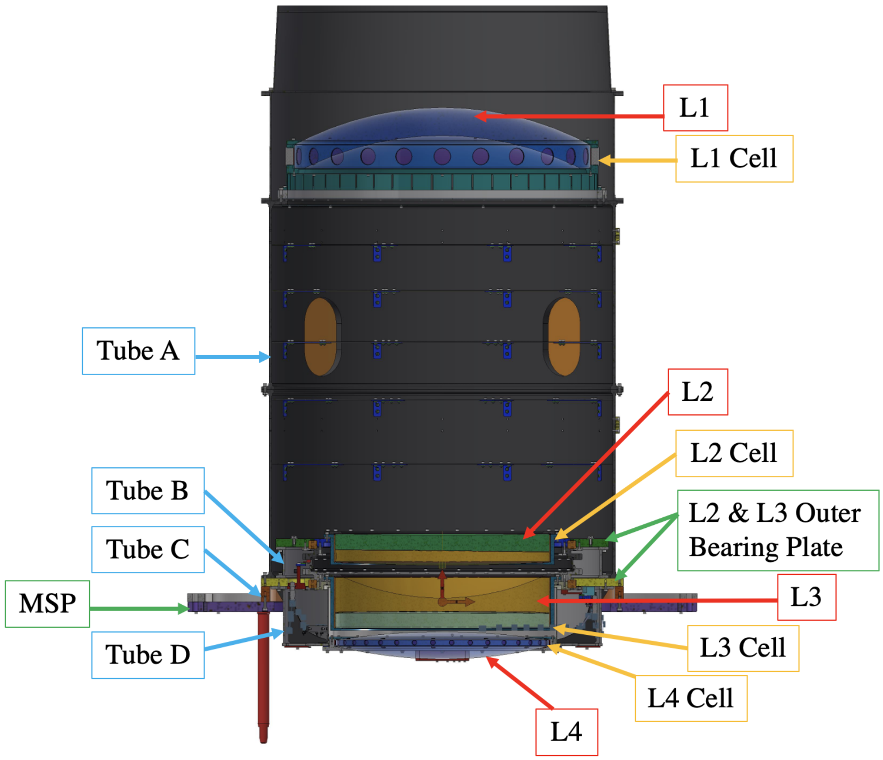

Figure 2: Labelled drawing of WFC with the main components.

and anti-reflection coated by Coherent in the USA, before being shipped to UCL for integration and assembly. Further discussion and details of the optical specifications can be found in Azais et al. 2016.[4]

Each lens is mounted in a lens cell which acts as an interface to the main barrel assembly. The ADC lens cells are mounted on interfaces (bearing plates) that can rotate as part of the ADC action. The Main Structural Plate (MSP) connects via a spacer to the telecope Cassegrain rotator.

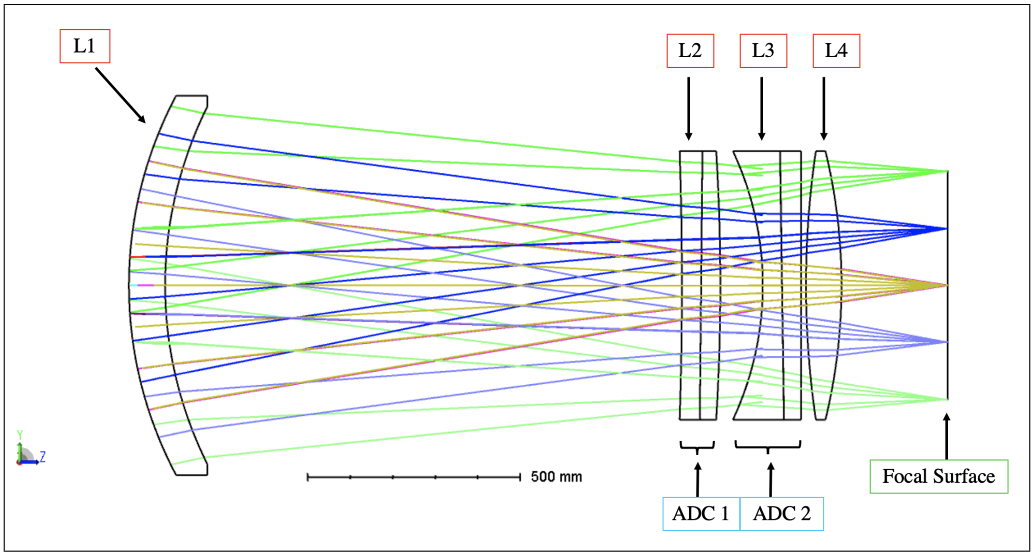

Figure 3: Optical layout of the WFC lenses, showing different focus positions for different field angles. This shows that all the lenses contribute in correcting the incoming light to produce high quality images across the focal plane.

1.3 General Assembly

The general assembly for the WFC is described in the flow diagram in figure 4. It has been broken down into 3 main stages. Pre-assembly describes the initial work done in order to allow the 'dry' assembly and the final assembly to be carried out. The 'dry' assembly describes the alignment and procedure that was followed without the lenses installed, this was carried out to give an indication of how the WFC would come together during the final assembly and how different surfaces mated with each other. The dry assembly also gave an opportunity to measure the position of the various surfaces which are then used in the derivation of the spacer thicknesses. During this measurement phase, all lens cells were aligned to a chosen axis and locked in location using insertable pins. The final assembly describes the final stages of putting the WFC together, integrating and aligning the different components.

2. ALIGNMENT STRATEGY

The alignment technique adopted was to use precision metrology of the components to position them to the required accuracy. The metrology methods used were a Faro gauge arm, and digital dial gauges coupled with a precision rotary table (see Figure 5 for image of dial guages). A check on the position of the lenses was made using a pencil beam laser alignment system (LAS). Dial gauges were used for surface flatness measurements as well as for centre runout measurements. The Faro gage arm was used for height measurements and to map out surfaces from which heights could be derived. A micrometer and vernier calipers were also used for sections of the assembly including the height measurements of the Tube A barrel and a laser displacement sensor (LDS) was used to measure the heights of the Room Temperature Vulcanised (RTV) rubber axial pads that supported the lenses when placed into their cells. A laser and camera system was also used to optically test the alignment of L1 and L4, details of which can be found in section 6.

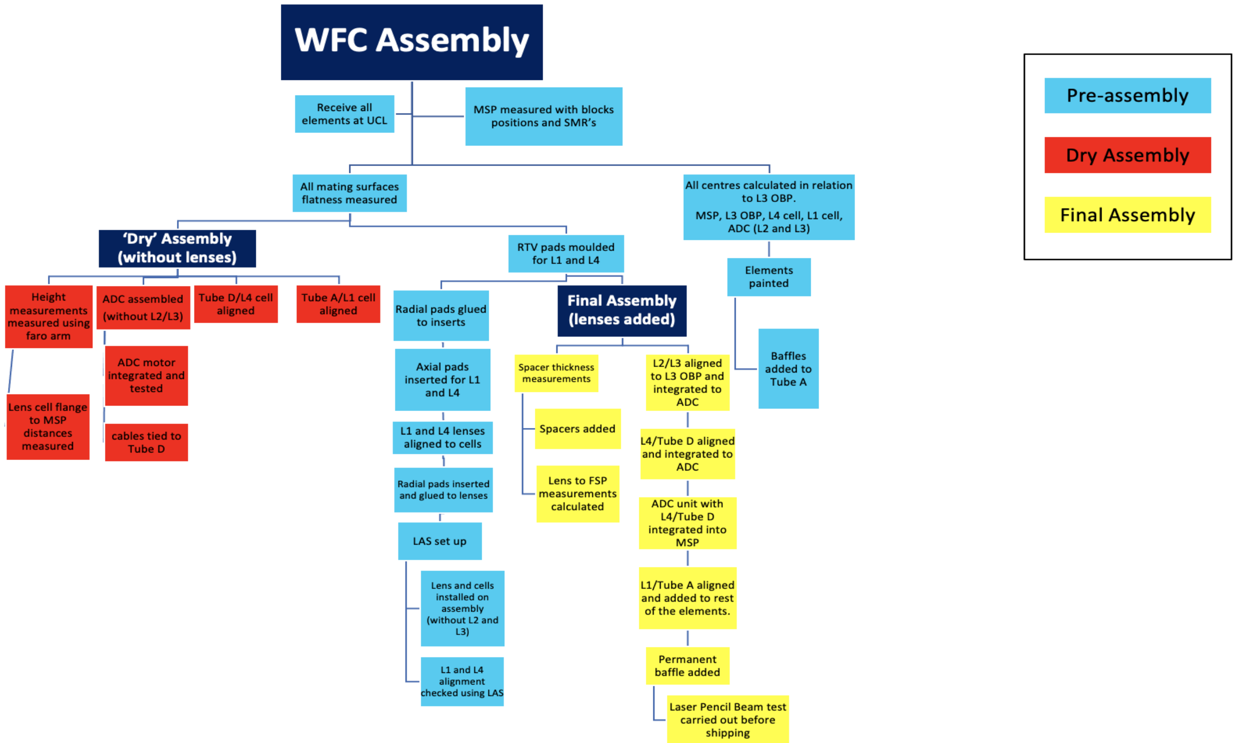

Figure 4: Flow diagram showing the general process of alignment and assembly for the WFC at UCL. The key on the right shows the different stages of assembly. This process chart shows the general procedure that was followed during the building and assembly of the WFC.

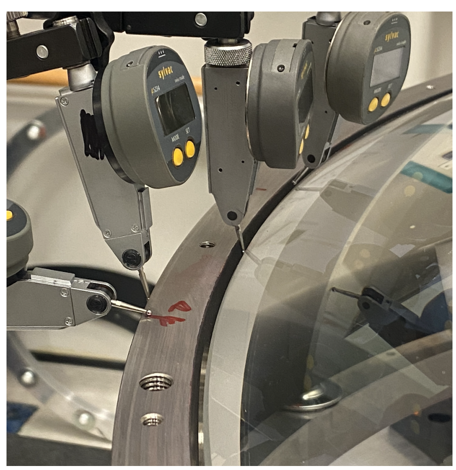

Figure 5: Image showing dial gauge measurements being taken of the both the L1 Lens and L1 cell.

Generally throughout the measurements, a 1-24 numbering system was used to mark angular position on each component, with each position corresponding to the evenly spaced bolt holes on the ADC bearing plates. The first position No.1 started at +X and the rotary table was turned anticlockwise until No.24. These positions were marked on the other elements so that the same numbering system remained consistent. In positions where the ADC coordinate/numbering system was not used, (mainly for the Main Structural Plate (MSP)) a 1-36 numbering system was used that again corresponded to evenly spaced holes on the MSP with No.1 stating at +X and the rotary table turning clockwise until No.36.

Firstly a reference position to align the components to in the system was established. This was chosen to be the centre position of the L3 outer bearing plate (OBP). The L3 OBP was chosen as this was a very circular surface and was in position during the majority of measurements when all the lens and barrel components were being measured. The measurement of the L3 outer bearing plate centre was performed using dial gauges on the outer diameter every time a new construction or alignment was carried out and the position of the WFC components referenced back to this position. During each re-measurement of the L3 outer bearing plate centre the plate was aligned such that its centre was within $10\mu m$ of the rotary table axis.

3. LENS-CELL AND BARREL ALIGNMENT

Each lens of the WFC had a requisite tolerance in which they were to be mounted into their respective lens cells. A full description of the optical prescription data can be found in Azais et al.(2016).[4] The lenses as shown in Figure 3, describe the optical lens layout with L1 being the largest lens at 0.9m in diameter and with the only aspheric surface, while the rest of the lenses (L2, L3 and L4) being 0.65m in diameter. UCL was responsible for the alignment and mounting of the L1 and L4 lenses into their respective cells, while Kiwistar were responsible for the mounting of the L2 and L3 lenses into their cells. UCL was then tasked with integrating all of these lenses with the ADC unit, and full assembly.

Accurate measurements of the elements interfaces and mating surfaces such as the cell flange surfaces were first measured. This included L1 cell flange which connected to Tube A, the L3 OBP plate surface which mated with the bottom of Tube A and finally the MSP. This measurement (of the flange positions) when combined with the crown to cell base measurements allowed a spacer thickness to be determined that would put the lens in the correct position relative to focal plane. All measurements were within $100\mu m$ of the nominal positions except for the L3 flange to MSP which had a deviation of $300\mu m$ from the nominal position (this was a manufacturing issue and had already been accounted for). These differences were adjusted by using machinable spacers and were added to the final assembly to ensure the distance from lens to the MSP/Focal Surface Plane (FSP) was consistent with the optical design.

3.1 Alignment of L2 and L3

L2 and L3 form the ADC unit and sit very close together. As L2 and L3 needed to be integrated into the ADC unit at UCL, the centre of the L2 and L3 inner bearings had to be established as this would be the rotary axis of the lenses. The L3 inner bearing plate inner diameter was measured in four positions each rotated by 90 degrees to understand how the centre changed as the bearing is rotated. From this, the centre was calculated by finding an average of the 4 positions. The same process was carried out for L2. Both the L2 and L3 inner bearing plates centre were aligned to each other to be within $\sim 20\mu m$ and aligned to the L3 outer bearing plate to within $\sim 40\mu m$.

Once the inner bearing centres were confirmed, the L2 and L3 lens surface and centres were measured (Figures 6 and 7). The L2 lens top surface was measured using the dial gauges and gave a runout of $\sim 500\mu m$. The initial measurements of L2 showed that it had $\sim 450\mu m$ of runout due to the wedge on the surface of L2, along with an additional $50\mu m$ of tilt relative to the cell flange. The L2 cell flange was them minimised and the top and bottom surfaces remeasured. The bottom surface was found to be tilted, giving a runout of $\sim 50\mu m$ (which happened to be in the same direction as the wedge). In the final set up, there was an additional $\sim 40\mu m$ of runout which is likely caused by the roughness of the mating surface. The L3 Lens top surface was measured in the same way using the dial gauges and gave a total runout of $48\mu m$). The centres of the L2 and L3 lenses in the ADC unit were found in the same way as the inner bearing centres, by rotating the bearing axis by $90°$(this time using the ADC motors that were tested at UCL) in 4 positions and finding an average.

(a) (b)

Figure 6: (a) Image showing the L2 lens flat surface being measured by a dial gauge while in the ADC unit. (b) Showing L2 lens and cell being lowered into the ADC unit. In this image, the L3 lens is also visible.

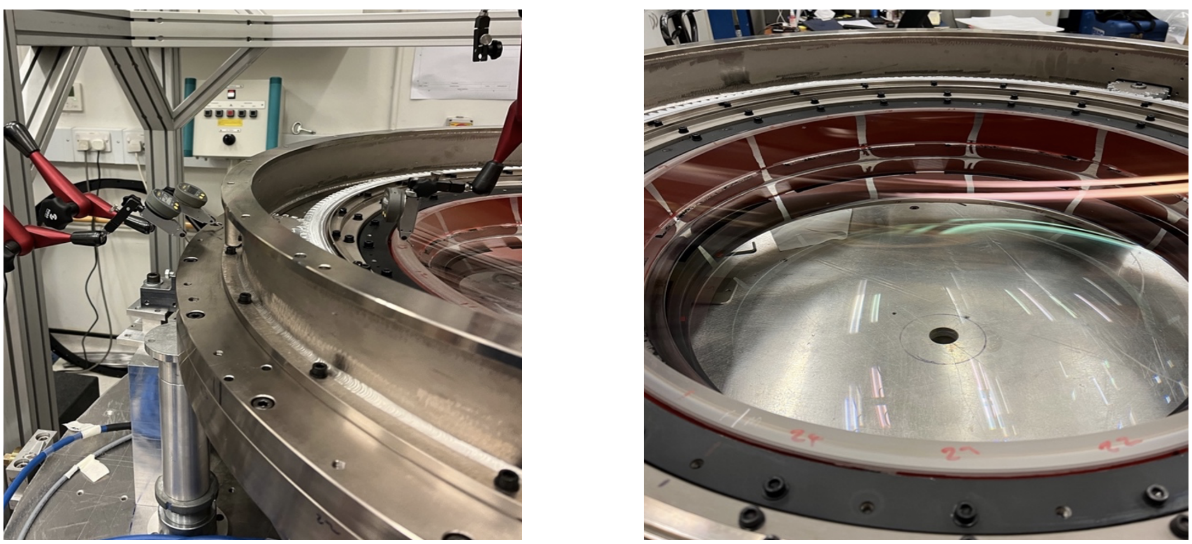

(a) (b)

Figure 7: (a) Image showing the L3 outer bearing plate and L3 lens being measured with dial gauges while supported on the rotary table using jacks. (b) Image showing a closeup of the L3 lens top surface in the ADC unit after measurements have been taken.

4. LENS TO CELL ALIGNMENT

4.1 RTV pads

After the initial lens cell flatness and surface measurements of the WFC elements were taken, the lenses were installed into their cells using Room Temperature Vulcanized rubber (RTV) pads as an interface between lens and cells. There are two sets of pads, axial and radial pads. The axial pads are glued (with a thin layer of RTV) into the cells. The action of the axial pads is to support the lens evenly and take up any unevenness in the cell support surface. The axial pads were installed such that their surfaces are on the same plane and parallel with the cell flange. During installation of the axial pads their surface position was verified using the Laser Displacement Sensor (LDS), and were found to be within $10\mu m$ (Figure 10).

The process of making the RTV involved mixing the RTV base compound and the curing agent together as shown in Figure 8, which was then degassed in a vacuum until the bubbling of the mixture stopped. The mixture was then placed into a mould (to ensure that all the pads were of uniform thickness) where it was then left for 24 hours to cure at room temperature. Once cured, it was cut out of the mould and into the correct size to be glued onto the lens cell inserts. The radial pads were then inserted through the cell and glued to the lens. The thickness of the pads were designed to make the lens-cell assembly essentially athermal to reduced induced stresses. This procedure was carried out for both the radial and axial pads for L1 and L4. Axial pads can be seen in Figure 9b.

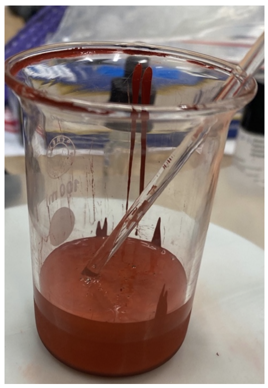

(a)

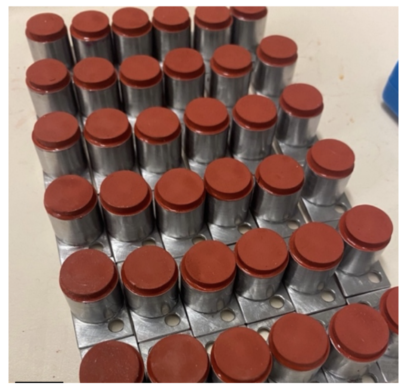

(b)

(c)

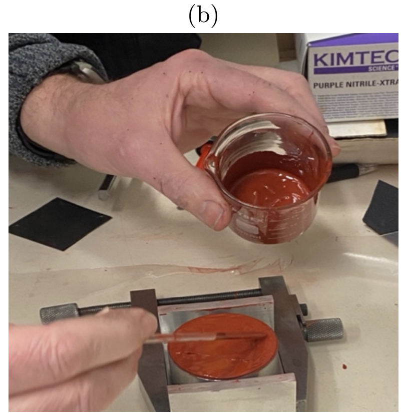

(d)

Figure 8: (a) image showing the RTV silicone rubber mixture before it would be placed into it moulds and left to cure for 24 hours. Images (b) and (c) show the L1 and L4 cell radial pads respectively, that have been glued to the radial inserts for L1 and L4. (d) shows the inserts being given another coat of the silicone rubber mixture before being glued to the lens.

(a)

(b)

Figure 9: (a)Image showing the process of scoring the surface of a cell where an RTV will be placed. The scratching of the cell aids in the RTV pad sticking to the cell. (b) Image showing the L4 cell with its 12 axial RTV pads (red squares) in place on the L4 angled surface, where the L4 lens will rest.

Figure 10: Image of the L1 axial pads being measured using the LDS, measurements were taken in the centre of the pad.

4.2 Lenses into cells

To insert a lens in its cell the lens is placed on a distributive load support system (whiffletree-like stage, shown in Figure 11). Extreme care was taken to space the support points of the whiffletree system so that the lens did not distort in anyway. More details of a similar process can be found in Doel et al.2012.[5]

Placing the lenses in their cells is a complicated and slow process. Raising the cell to the supported lens ensuring the cell was kept level at all sides by slowly raising each jack to the correct height until the axial pads within the cell meet the lens. The larger jacks move the lens cell into place by carrying out larger movements ($\sim 100 \mu m$). Once the lens cell was close enough to the lens (within 2mm), the jacks were replaced with aluminium posts and precision screw jacks to raise the lens cell in finer incremental steps (5-10 μm). The tip and tilt of the lens was controlled with the same precision screw jacks. A dial gauge was used to ensure all sides were raised equally until the pads began to make contact with the lens. At this stage, the positions of both the lens and the cell were measured again to establish their positions before the radial pads were glued in place.

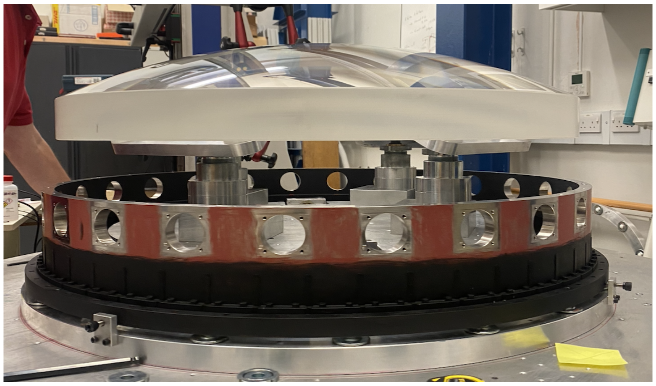

(a)

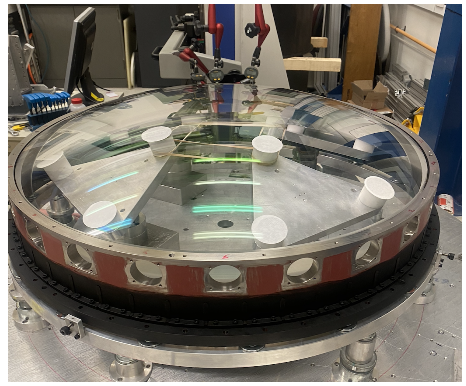

(b)

Figure 11: (a) L1 lens being supported on the whiffletree structure on the rotary table before being put into its cell. (b) L1 lens resting on the axial pads in L1 cell before the RTV pads are inserted (the white visible circles shown are where the whiffetree structure is supporting the lens).

To attach the radial pads the following procedure was used. The radial pads on their inserts were first were screwed in but not glued to the lens but instead had a paper of a suitable thickness ($\sim 40 \mu m$)to take up the gap between the RTV of the radial pads and the lens outer diameter. This locked the entire system in position. Opposite pairs of the radial pads were removed and the glass was primed before the freshly RTV glued pads were reinserted. Two pairs of opposing pads at 90° to each other were glued in at a time and allowed to cure, this was continued until all pads were inserted to ensure minimal movement in any one direction of the lens until the process was complete and the lens was fully glued to the cell. The same procedure was carried out for both L1 and L4.

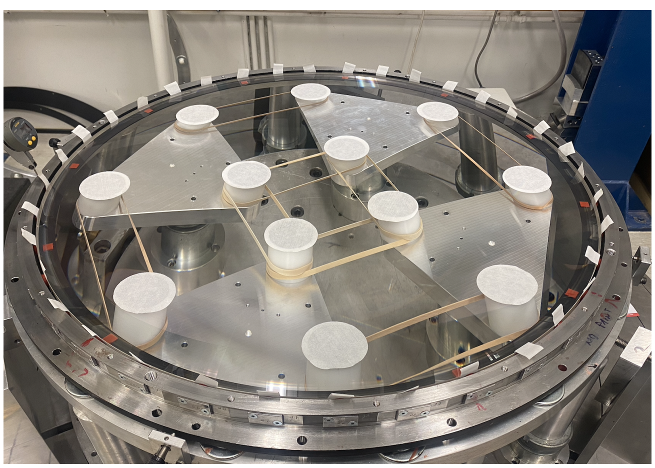

(a)

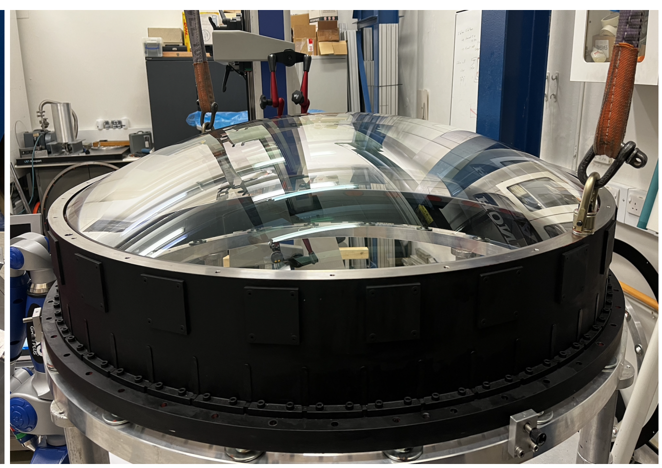

(b)

Figure 12: (a) L4 lens in its cell with the 40 µm paper stopping the RTV pad inserts from touching the lens before they get glued in place. (b) Final assembly of L1 lens in L1 cell after RTV pads have been inserted and rest of the L1 cell has been painted black.

All lenses were put into their cells to minimise the bottom surface runout (bottom surface refers to the surface closest to the FSP and the surface that), so that a wedge (if any) would be expressed on the top surface. The L1 lens was deliberately offset in the cell by $\sim 70 \mu m$ in X and $\sim 30 \mu m$ m in Y to ensure the L1 asphere is centered and flattened, which left a runout of $\pm 40\mu m$ on the top surface. When put into the full final assembly, this changed to $\pm 80\mu m$ (Figure 13). This additional runout expressed when in final assembly could also be explained by both the variation in the flatness of the surfaces when mated and also a projection effect, as L1 is sitting on-top of the tall barrel, if there were a few microns tilt at the bottom, this could express an increased runout on the top. This increased runout is due either to lens decentre or a tilt of the lens - but is well within tolerance.

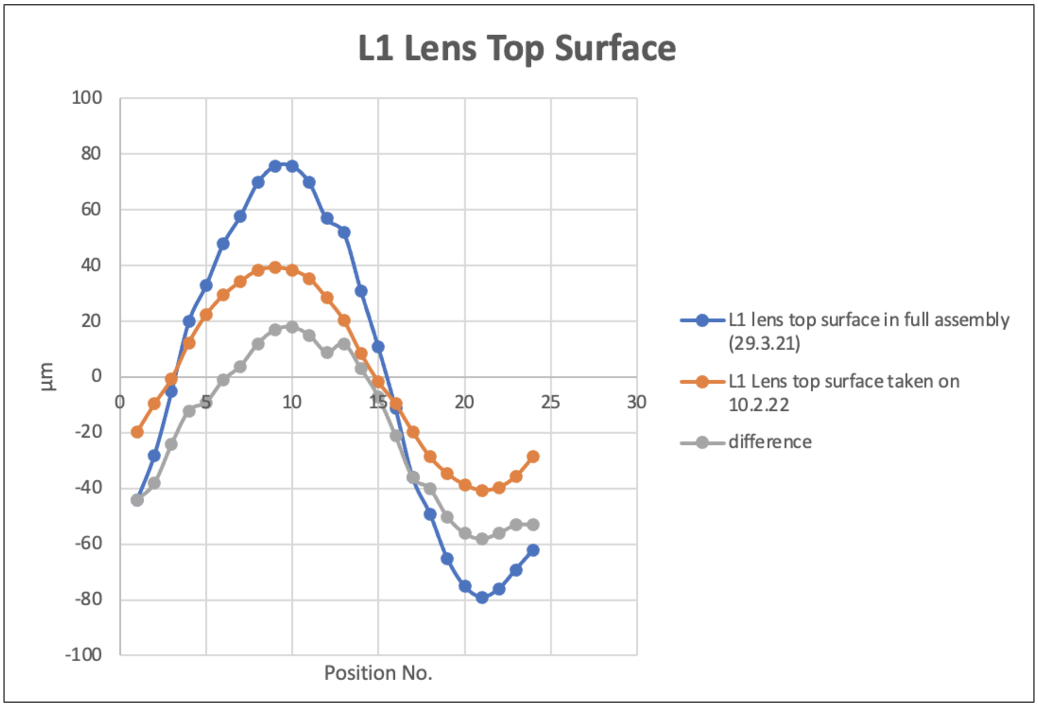

Figure 13: L1 lens top surface variation comparing flatness before being put into full assembly and after, along with the difference between them. Measurements taking using a dial gauge, showing the assembled L1 lens top surface to be within $\pm 80\mu m$.

5. LASER ALIGNMENT TEST

5.1 Set up

As an additional check to the contact metrology measurements for the alignment of the lenses, a laser alignment system (LAS)[5] was built at UCL to test the relationship between L1 and L4 in the assembled system without the ADC optics (see Figure 14 and 18). The WFC was assembled in two variations on the rotary table to cater for the tests to be carried out on L1 and L4 (one system with L1 and L4 together, and another system with just L4). Prior to the lenses being put in, tests were carried out using a retro-reflector and a corner-cube to check the parallelism and centring of the laser on the rotary table. Once the system to be tested was set up and aligned with the L1 and L4 lenses in position, it was then rotated through 360° taking measurements at every 90°. Two cameras were installed, one below the rotary table to capture the through beam of the laser and one above, to capture the reflected beam. This test was carried out to test 4 key elements; the through beam of L4, the reflected beam of L4, the through beam of L1 and L4 together and finally the reflected beam of L1. The main aim of these tests was to check that L1 and L4 were aligned to within the measured uncertainties, that L1 was consistent with L4 when assembled in the barrel and that the results coordinated with the contact metrology measurements. Both the L1 and L4 centroids found with the LAS system confirmed that our centres and tilts were well within the accepted tolerances for both L1 and L4.

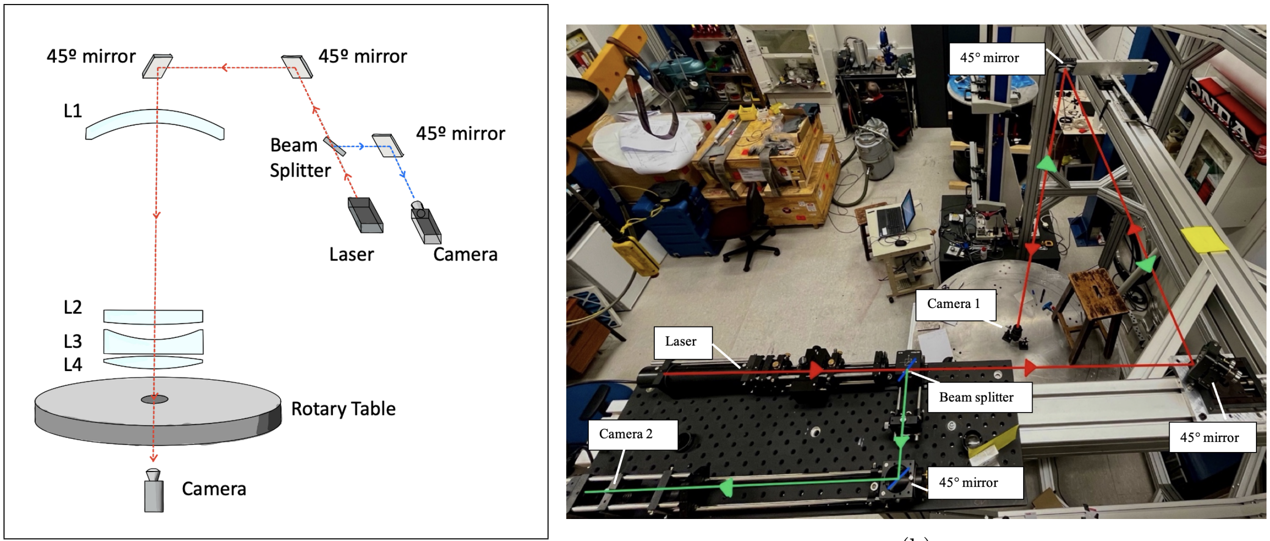

(a) (b)

Figure 14: (a) Labelled schematic of the Laser Alignment System used to test the optics. The red arrow indicates the path the laser beam takes, hitting a two 45°mirrors before passing through the WFC system, the rotary table and through to the camera for the through beam. The blue arrows indicate the reflected path of the laser beam going into the 2nd camera. (b) Showing a photo of the LAS set up in the lab.

6. ALIGNMENT RESULTS AND FINAL ASSEMBLY

Tests were carried out at each stage of the final assembly to ensure everything was consistent with our previous measurements. 'Loctite 243' was applied to the bolts before insertion to ensure to ensure bolts were secure and to prevent loosening. Images of final assembly process can be found in the Appendix A.

6.1 Off-axis Laser Pencil Beam

After final assembly was complete, a Laser Pencil Beam (LPB) Tool was used to test the optics of the WFC for pre and post delivery to Leibniz Institute for Astrophysics, Potsdam (AIP). The laser was set up as shown in Figure 16. An off-axis laser beam was sent through the system and the reflection of each lens surface was captured by a built-in camera which determined the position of each lens. On arrival to AIP, the same test was carried out to determine if there was any movement of the optics during transportation. The WFC was successfully delivered and all lenses maintained to be within measurement uncertainties.

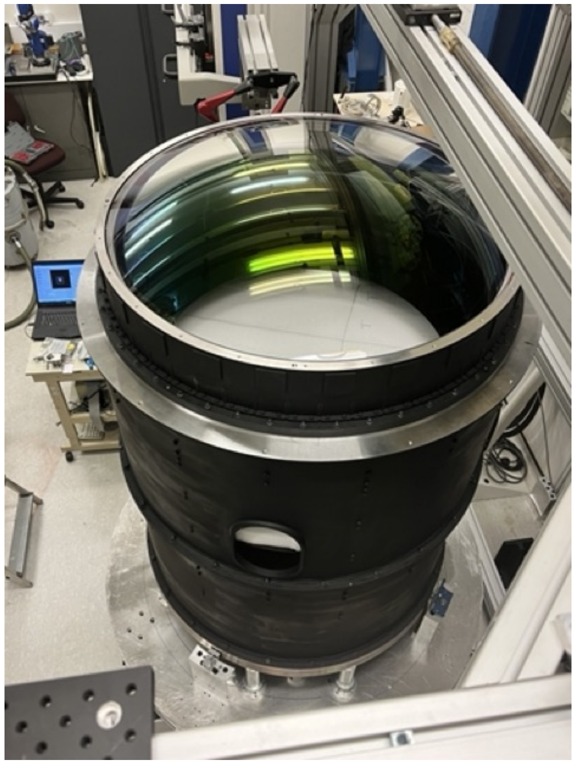

Figure 15: Top-down view of the WFC assembly on the rotary table (without L2 and L3 inserted). L1 lens is shown at the top and is where the laser enters first. Just below L1 there is polystyrene foam that was added to stop any reflections from the L4 lens interfering with the L1 reflected beam, this was also used to stop things falling onto the L4 lens.

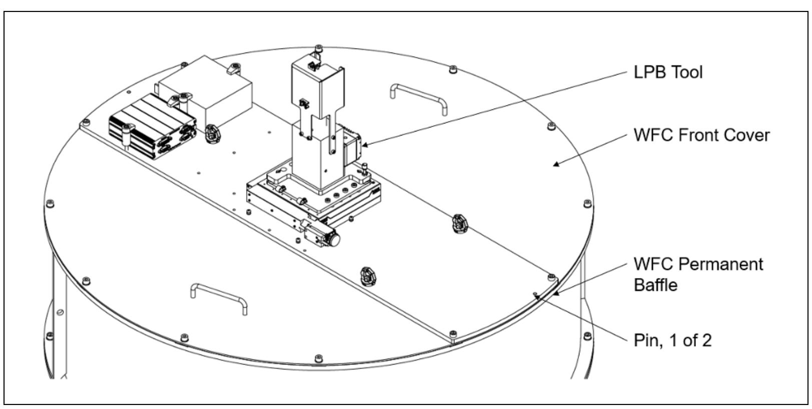

(a)

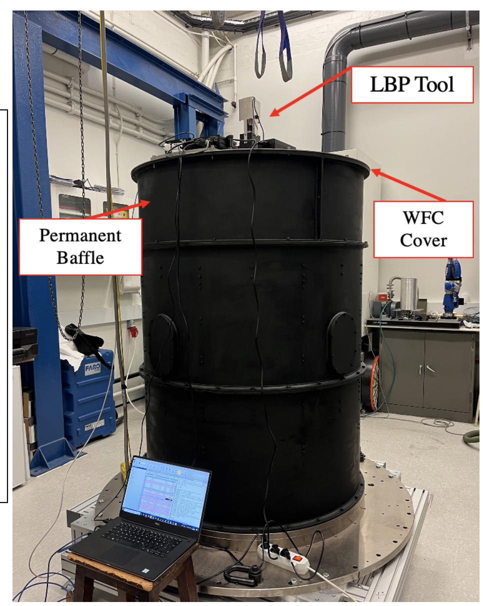

(b)

Figure 16: (a) Schematic of the LPB Tool that was used to test the movement of the lenses pre and post delivery to AIP. (b) Image of the LPB tool during testing.

6.2 Lens Centres

The final lens centre positions for each lens in the final set up are shown in the table below. All lenses were compared to the L3 OBP as this was our reference centre. All lenses fall within within the decentering tolerances given for each lens.

Table 1: Alignment results.

Lens	Lens decentre (X,Y) (μm)	Tolerance (X,Y) (μm)
L1	(-41.75, 15.13)	200
L2	(19.51, -16.04)	1000
L3	(6.79, 7.10)	100
L4	(22.27, -7.65)	200

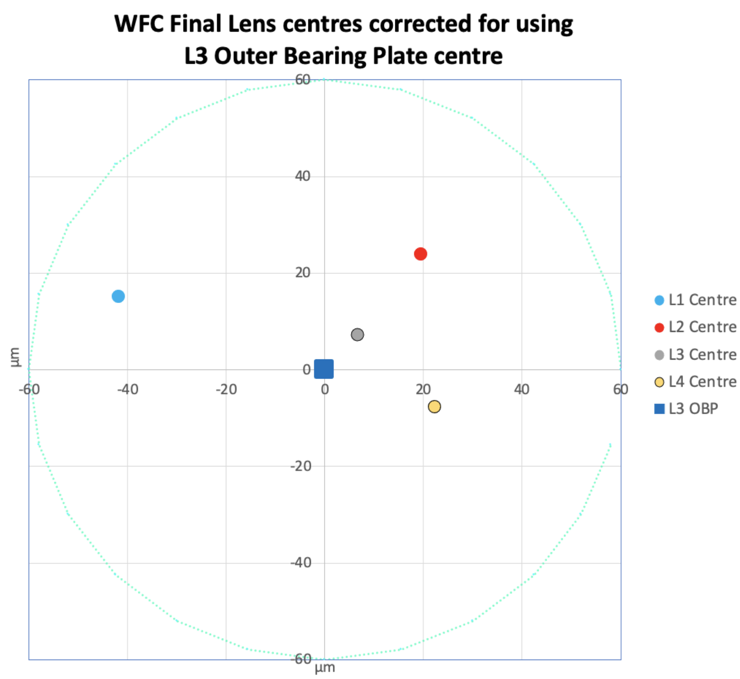

Figure 17: Plot showing the WFC lens centres after installation in barrel relative to the target centre of the L3 OBP.

6.3 Lens tilts

As previously described each lens's bottom surface runout was minimised when put into its cell, this left a runout on the top surface. These runouts on the top surfaces of each lens are expressed in the table below. The table describes the initial lens surface variations in the cell pre-assembly after the lenses have been mated into their cells and the lens surface variations after the lenses have been put into the full WFC assembly. The difference between the two variations was calculated (this accounted for positional variation also) and the tilt angle found. All lens tilts lay well within the given tolerances.

Table 2: The WFC Lens tilts calculated from the lens surface runouts.

Lens	Initial lens surface variation (μm)	Lens surface in full assembly	Change in variation (μm)	Tilt angle (μrad)	Tilt Tolerance ($\pm\mu rad$)
L1	80	155	75	83.33	785
L2	489	647	78.46	83.33	945
L3	8	47	75	60	95
L4	67	68	19	29.23	142

7. CONCLUSION

All lenses were successfully installed into the corrector, without damage and well within the allotted tolerance. The corrector was successfully shipped to AIP with no movement of the optics during transportation and will begin integration with AESOP before continuing its journey to the telescope.

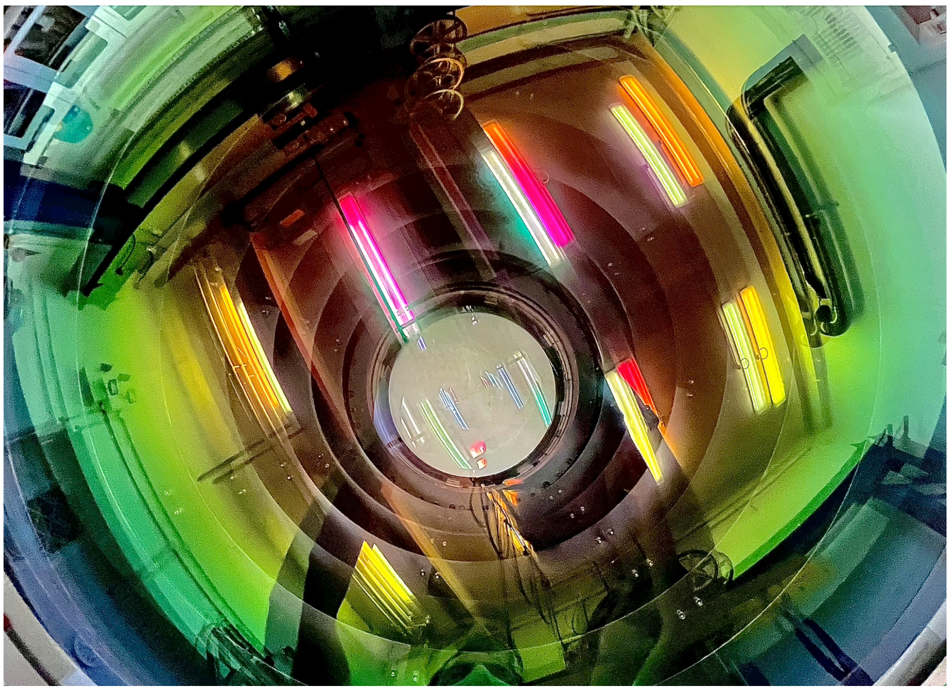

Figure 18: Top-down view of the WFC assembly on the rotary table (without L2 and L3 inserted). L1 lens is shown at the top and is where the laser enters first. Just below L1 there is polystyrene foam that was added to stop any reflections from the L4 lens interfering with the L1 reflected beam.

APPENDIX A. ASSEMBLY PROCESS

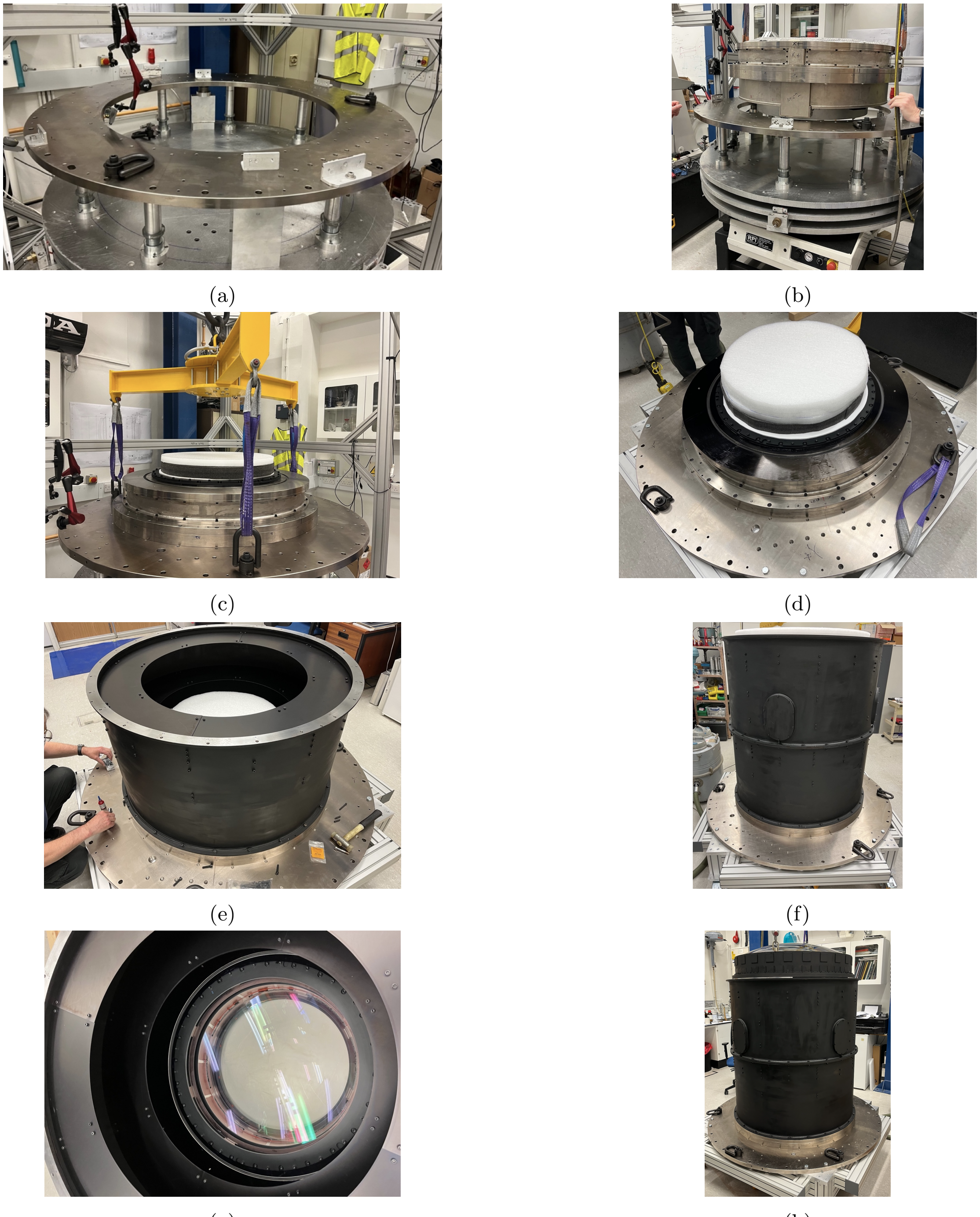

Figure 19: Final assembly of the WFC after all lenses have been aligned to the system. Measurements were taken at each stage to ensure alignment had not changed. (a) Main Structural Plate (MSP) (b)ADC being lowered into MSP. (c) ADC unit integrated with MSP. (d) L2 bearing plate blackened surface in ADC unit. (e) Tube A part (ii) integrated with MSP and ADC. (f) Tube A fully integrated. (g) Look down at the internal baffles of Tube A. (h) Fully assembled WFC with L1 integrated.

REFERENCES

[1] Ellis, R. S., Bland-Hawthorn, J., Bremer, M., Brinchmann, J., Guzzo, L., Richard, J., Rix, H.-W., Tolstoy, E., and Watson, D., "The future of multi-object spectroscopy: a eso working group report," (2017).

[2] de Jong, R. S., Barden, S. C., Bellido-Tirado, O., Brynnel, J. G., Frey, S., Giannone, D., Haynes, R., Johl, D., Phillips, D., Schnurr, O., Walcher, J. C., Winkler, R., Ansorge, W. R., Feltzing, S., McMahon, R. G., Baker, G., Caillier, P., Dwelly, T., Gaessler, W., Iwert, O., Mandel, H. G., Piskunov, N. A., Pragt, J. H., Walton, N. A., Bensby, T., Bergemann, M., Chiappini, C., Christlieb, N., Cioni, M.-R. L., Driver, S., Finoguenov, A., Helmi, A., Irwin, M. J., Kitaura, F.-S., Kneib, J.-P., Liske, J., Merloni, A., Minchev, I., Richard, J., and Starkenburg, E., "4MOST: the 4-metre Multi-Object Spectroscopic Telescope project at preliminary design review," **9908**, 99081O (Aug. 2016).

[3] de Jong, R. S., Bellido-Tirado, O., Chiappini, C., Depagne, E., Haynes, R., Johl, D., Schnurr, O., Schwope, A., Walcher, J., Dionies, F., and et al., "4most: 4-metre multi-object spectroscopic telescope," *Ground-based and Airborne Instrumentation for Astronomy IV* (Oct 2012).

[4] Azais, N., Barden, S., Smith, G., Jones, D., Delabre, B., and Egron, S., "Wide field corrector for 4most: design details and maiv processes," (Jun 2016).

[5] Doel, P., Brooks, D., Antonik, M. L., Flaugher, B. L., Stefanik, A., Kent, S. M., Gutierrez, G., Cease, H. P., Abbott, T. M., Walker, A. R., DePoy, D. L., Bernstein, R. A., and Worswick, S., "Assembly, alignment, and testing of the DECam wide field corrector optics," in [*Ground-based and Airborne Instrumentation for Astronomy IV*], McLean, I. S., Ramsay, S. K., and Takami, H., eds., *Society of Photo-Optical Instrumentation Engineers (SPIE) Conference Series* **8446**, 84466F (Sept. 2012).